World Academy of Science, Engineering and Technology
International Journal of Physical and Mathematical Sciences
Vol:11, No:3, 2017

Optical and Dielectric Properties of Self-Assembled 0D Hybrid Organic-Inorganic Insulator

S. Kassou, R. El Mrabet, A. Belaaraj, P. Guionneau, N. Hadi, T. Lamcharfi

***Abstract*—**The organic–inorganic hybrid perovskite-like $[C_6H_5C_2H_4NH_3]_2ZnCl_4$ (PEA-$ZnCl_4$) was synthesized by saturated solutions method. X-ray powder diffraction, Raman spectroscopy, UV-visible transmittance, and capacitance meter measurements have been used to characterize the structure, the functional groups, the optical parameters, and the dielectric constants of the material. The material has a layered structure. The optical transmittance (T %) was recorded and applied to deduce the absorption coefficient (α) and optical band gap (Eg). The hybrid shows an insulator character with a direct band gap about 4.46 eV, and presents high dielectric constants up to a frequency of about 10^5 Hz, which suggests a ferroelectric behavior. The reported optical and dielectric properties can help to understand the fundamental properties of perovskite materials and also to be used for optimizing or designing new devices.

***Keywords*—**Dielectric constants, optical band gap (Eg), optical parameters, Raman spectroscopy, self-assembly organic inorganic hybrid**.**

I. Introduction

RECENT years have witnessed extensive development on organic-inorganic hybrid perovskites, notably from both experimental and theoretical scientific communities, due to their interesting structural, optical and thermal properties [1]–[20]. These make them promising candidates for application in photovoltaic (PV) and related optoelectronic devices [21]–[27]. Their structure consisting of alternating layers between organic and inorganic components, provides substantial opportunities with respect to both combining useful attributes of organic and inorganic components, and gives new properties as result of the interface between the two entities. The optical properties like band gap present one of the interesting features of this kind of compounds. They construct a multi-quantum well energy band: the inorganic anion constructs the well deep of the multiple quantum wells because the energy bands near the Fermi level is mainly governed by the orbital of inorganic atoms, while the organic cation plays the role of a potential barrier [28], and this leads to new multifunctional materials. The visible-ultraviolet light absorbed by the sample gives information about the transparency which is very essential in many optoelectronic applications [29]–[31]. In this work, we report the synthesis, optical and dielectric features of the hybrid PEA-$ZnCl_4$ compound. The powder X-Ray diffraction has been used for a crystallographic characterization. The RAMAN spectroscopy was used to determinate the functional groups of the compound. The transmittance, the absorption coefficient, the optical band gap energy, and the refractive index were determined by UV-visible spectroscopy. The capacitance meter measurements were used to deduce the dielectric constant and dielectric loss of the studied materials.

A. Belaaraj is with the Laboratoire Physique des Matériaux et Modélisation des Systèmes CNRST-URAC08, Université Moulay Ismail, Faculté des Sciences Département de Physique, B.P. 11201, Zitoune, 50000 Meknes, Morocco (e-mail: a.belaaraj@fs-umi.ac.ma).

S. Kassou and R. El Mrabet are with the Laboratoire Physique des Matériaux et Modélisation des Systèmes CNRST-URAC08, Université Moulay Ismail, Faculté des Sciences Département de Physique, B.P. 11201, Zitoune, 50000 Meknes, Morocco.

P. Guionneau is with the CNRS, Univ.Bordeaux, ICMCB, UPR 9048, F-33600 Pessac, France.

N. Hadi and T. Lamcharfi are with the Laboratoire Signaux, Systèmes et composants, USMBA, FST Fez, B.P. 2202, Morocco.

II. Experimental

A. Synthesis and Powder X-Ray Diffraction

The organic inorganic hybrid perovskite PEA-$ZnCl_4$ was synthesized by saturated solutions method. The starting materials were weighed in stoichiometric proportion and dissolved in a minimum quantity of water/ethanol (1:1 in ratio) as solvent, and few drops of HCl (37%) were added to protonate $C_6H_5C_2H_4NH_2$. On the other hand, $ZnCl_2$ was dissolved in 3 ml of water/ethanol. White polycrystalline powder was obtained after few hours when mixing two saturated solutions. The crystalline phase purity of the compound was confirmed comparing the powder X-ray diffraction (P- XRD) pattern to the simulated pattern from its structure as shown in Fig. 1.

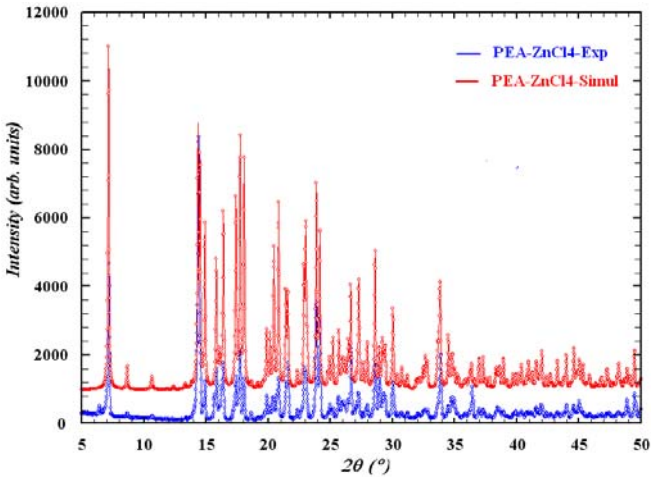

Fig. 1 Experimental and simulated X-Ray diffraction patterns of PEA-$ZnCl_4$

B. Characterization Methods

UV-vis diffuse reflectance and transmittance spectroscopy measurements were recorded on a Jasco v-570 spectrophotometer with an integrating sphere over the spectral range 200-2000 nm. A barium sulfate ($BaSO_4$) plate was used as the standard (100 % reflectance) on which the finely ground sample from the crystal was coated. Raman spectra measurements in the frequency range 200-3200 cm^{-1} were carried out on a LabRAM Horiba Jobin Yvon spectrometer equipped with a CCD detector and a HeNe laser (532 nm) at 5 mW. The dielectric measurements were performed on a pellet of about 10 mm in diameter and 0.8 mm in thickness, using an inductance capacitance resistance (LCR) bridge HP, 4284A in the frequency range of 100 Hz to 2 MHz. All measurements were performed at room temperature.

III. Results and Discussion

The PEA-$ZnCl_4$ compound crystallizes in the monoclinic system with P21/c space group, and the cell parameters a=7.449(2) Å, b=24.670(3) Å, c=11.187(2) Å, β=91.762(5)° and Z= 4 [32]. The structure is consisted of isolated tetrahedral $[ZnCl_4]^{2-}$ in 0D dimension where each Zn ion is coordinated by four chlorine atoms. The cohesion of the structures is established by hydrogen bonding between organic and inorganic components and by Van Der Waals interactions between organic layers (Fig. 2).

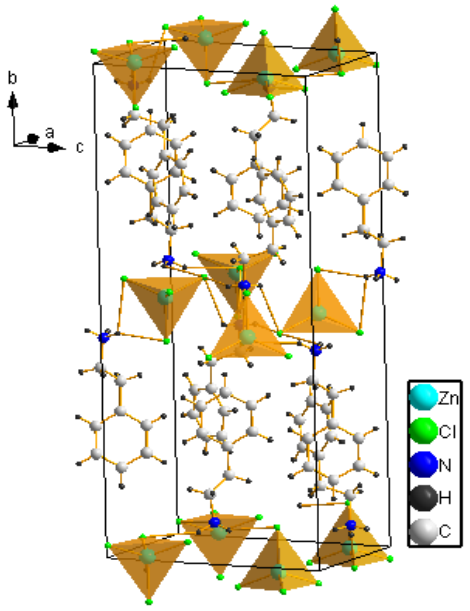

Fig. 2 Overall view of PEA-$ZnCl_4$ crystal structure [32]

A. Raman Spectra

The Raman spectrum of PEA-$ZnCl_4$ (Fig. 3) was recorded at room temperature in the range of 400-3500 cm^{-1}. The attribution of all bands for the material is based on comparison with some homologous compounds [33]–[37]. The frequency band 3058 cm^{-1} is assigned to the asymmetric stretching $\nu_{as}(CH_3)$ aromatic mode. The observed band at 2740 cm^{-1} is related to symmetric $\nu_{sym}(NH^+)$ mode. However, the observed bands at 1608 cm^{-1} and 1516 cm^{-1} are assigned to the symmetric stretching $\nu_{sym}(CH_3)$ and to deformation δ(NH) respectively. The band appearing at 1441 cm^{-1} is ascribed to symmetric stretching $\nu_{sym}(CH_3)+\nu_{sym}(CH_2)$ modes. At frequency 1216 cm^{-1}, a deformation in plan $\omega_{sym}(CH_3)$ appears. The medium band appearing at 1149 cm^{-1} is assigned to the twisting $t(CH_2)$. The band located at 1003 cm^{-1} is attributed to the deformation δ(C = C) aromatic mode. At lower frequencies, the rocking mode $\rho(NH_3)$ is observed at 483 cm^{-1}. The asymmetric and symmetric stretching vibrations of (Zn-Cl) appear at 283 cm^{-1}.

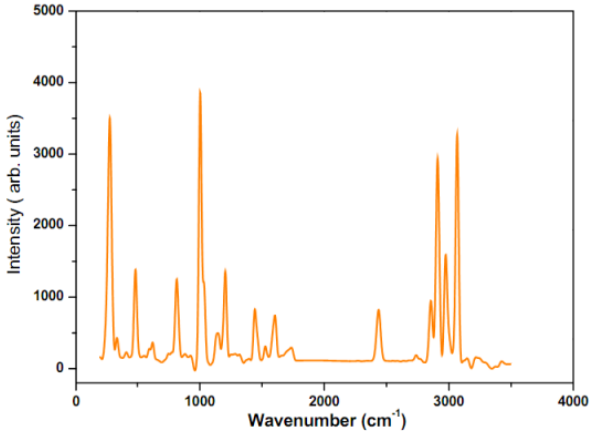

Fig. 3 Raman spectrum of PEA-$ZnCl_4$

B. Optical Properties

To determine the operative transparency range, the UV-visible transmittance spectrum was recorded in the range of 200-2000 nm. As shown in Fig. 4, we can note that the studied material is optically transparent up to about 300 nm. This transparency remains uniform over the visible region, which indicates that the compound has a high optical homogeneity. The lower cutoff wavelength is found to be about 280 nm. In the infrared range, the sample presents a variation curve. These frequency bands are attributed to the vibrational modes of the organic part. Therefore, the material could be of importance in new generation optoelectronic devices.

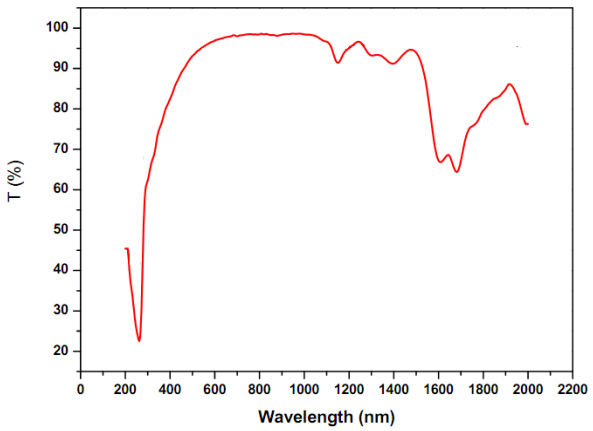

Fig. 4 UV-visible transmittance spectrum of PEA-$ZnCl_4$

The optical constants of such material play critical roles to adapt the needs of technological components [38], [39]. The optical absorption coefficient (α) and the band gap energy (Eg) are the most pivotal parameters. The first one was calculated from the relation: α= (2.303 log (1/T))/d where T is the transmittance, and d is the thickness of the sample. The corresponding variation versus wavelength is depicted in the Fig. 5. It can be seen that this coefficient shows an absorption edge at about 278 nm, and then decreases as the wavelength increases. The shape of the absorption coefficient curves reveals that the material exhibits a direct allowed transition [40]. The band gap parameter is related to the absorption coefficient by the relation $\alpha h\nu = A(h\nu - Eg)^n$ [41] where hν is the photon energy, A is a constant, Eg is the band gap energy, α is the optical absorption coefficient, and n is an index parameter which reflects the nature of electron transition in the absorption process (n=1/2, 3/2 for a direct transition and n=2, 3 for allowed indirect transition).

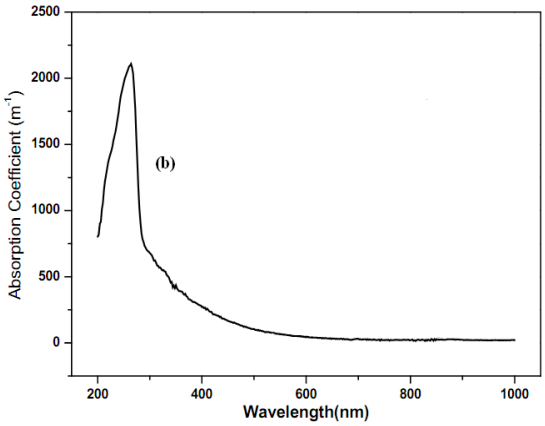

Fig. 5 Optical absorption coefficient (α) for PEA-$ZnCl_4$

The intercept on x (hν) axis, corresponds to zero absorption coefficient in Tauc plot (Fig. 6) and gives the optical band gap energy value. The observed value 4.46 eV is wider than that of a similar compound based on $CuCl_4$ [42], which is about 2.3 eV, and it implies the insulating behavior of the material.

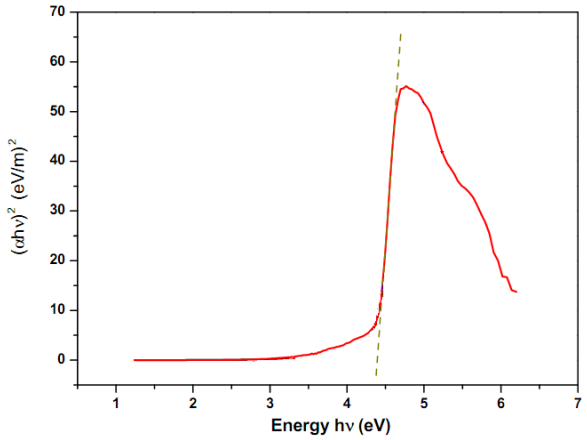

Fig. 6 Tauc plot of $(\alpha h\nu)^2$ vs photon energy (hν) for PEA-$ZnCl_4$

The refractive index value (n) was calculated using Fresnel's coefficient expression [43], [44]: $n = (R+1)/(R-1) + [(1+R)/(R-1)^2 - (1-k^2)]^{1/2}$ where R is the reflectance, and k is the extinction coefficient excerpt from $k = \lambda\alpha/4\pi$ equation in the visible region for the material. Fig. 7 reveals that the refractive index decreases with the increase of wavelength. The calculated index value for PEA-$ZnCl_4$ at 400 nm (n= 2.33), is in good agreement with the refractive index of the ferroelectric material $Sr_{0.61}Ba_{0.3}$ Nb_2O_6 (2.35 at 400 nm) [45], therefrom it predicts the ferroelectric behavior of the studied material.

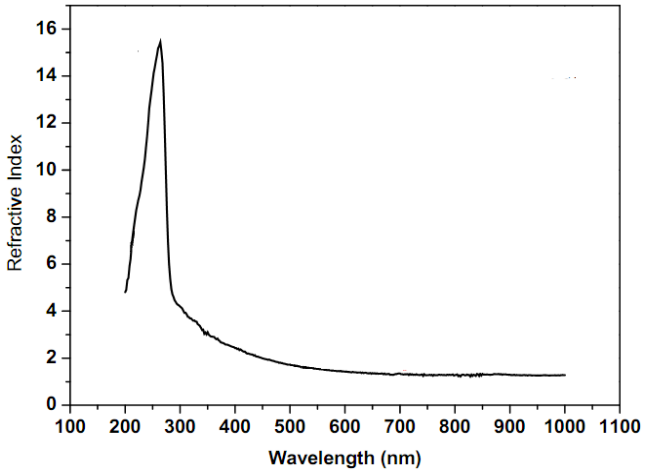

Fig. 7 Refractive index (n) for PEA-$ZnCl_4$

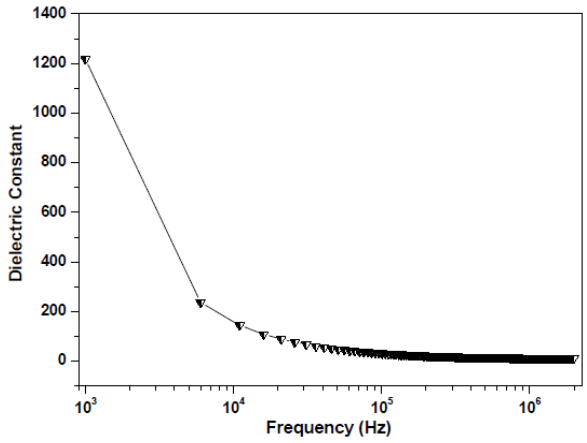

Fig. 8 Dielectric constant for PEA-$ZnCl_4$

C. Dielectric Properties

The dielectric behavior of the metal-halide perovskites is related to their structural features and reveals the effect of microstructure on the polarons [46]. The existence of the organic bilayer in PEA-$ZnCl_4$ leads to use this material in high efficiency energy storage devices [47]. Fig. 8 shows the dielectric constants for the studied compound, recorded at room temperature as a function of frequency. We can note that the dielectric constant presents high values up to about 10^5 Hz, which predicts a ferroelectric behavior of the material, and decreases exponentially with frequency due to a normal behavior of polar dielectric. At low frequency, the space

charge polarization is more predominant, and therefore, decreases until a point of space charge where cannot endure and comply with field-applied externally. As consequently the polarization decreases which led to diminishing of dielectric constant values [48]. The dielectric loss reflects the contribution of both parts intrinsic and extrinsic (crystal structure and imperfections in the crystal) on polarons. The lower values of the dielectric loss shown in Fig. 9 reveal the good quality of the crystal with less defects, which makes this parameter an appropriate candidate for the fabrication of optoelectronic materials [49], [50].

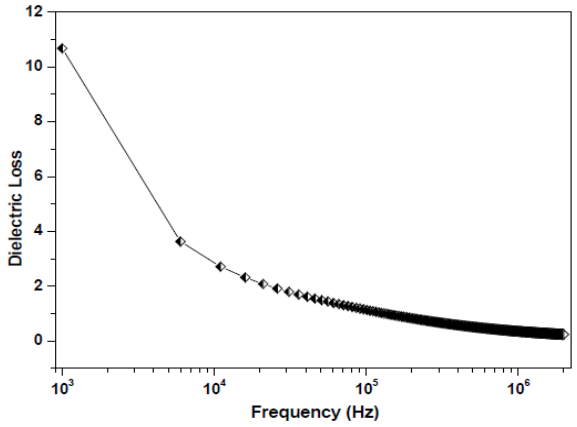

Fig. 9 Dielectric loss for PEA-$ZnCl_4$

IV. Conclusion

The organic-inorganic hybrid perovskite-like $[C_6H_5C_2H_4NH_3]_2ZnCl_4$ material was synthesized by saturated solutions method. The vibrations modes of the functional groups were identified by Raman studies. The transmittance in the visible region was obtained from UV-vis spectroscopy. The observed optical band gap energy value 4.46 eV, deduced from Tauc plot for the studied material suggests that the material exhibits a dielectric behavior. The value of refractive index at 400 nm which is 2.33 implies that the hybrid is part of a new family of ferroelectric materials. The dielectric constants and dielectric loss are affected by the nature of structure. The lower value of dielectric loss reveals the contribution of crystal structure and imperfections in the crystal on the polarons. However, the obtained values of dielectric constants reflect the contribution of all polarizability components such as space charge, dipolar, ionic, and electronic in the ferroelectric behavior of the material.

References

[1] D. B. Mitzi, "Synthesis, structure, and properties of organic-inorganic perovskites and related materials." *Prog. Inorg. Chem.*, vol. 48, pp. 1-121, 2007.

[2] S. Zhang,G. Lanty, J. S. Lauret, E. Deleporte, P. Audebert and L. Galmiche, "Synthesis and optical properties of novel organic–inorganic hybrid nanolayer structure semiconductors." *Acta. Mater.,* vol. 57, pp. 3301-3309, 2009.

[3] D. Ionescu, I. B. Ciobanu and I. Radinschi, "Frequency resonant behaviour of the effective permittivity for a polyvalent liquid crystal in microwave range." *J. Optoelectron. Adv. M.*, vol. 9, pp. 2608-2616, 2007.

[4] S. Zhang, P. Audebert, Y. Wei, J. S. Lauret, L. Galmiche and E. Deleporte "Synthesis and optical properties of novel organic–inorganic hybrid uv (R–NH 3) 2 PbCl 4 semiconductors." *J. Mater. Chem*., vol. 21, pp. 466-474, 2011.

[5] M. F. Mostafa and S. S. El-Khiyami, "Crystal structure and electric properties of the organic–inorganic hybrid: $((CH_2)_6(NH_3)_2)ZnCl_4$." *J. Solid State Chem.*, vol. 209, pp. 82-88, 2014.

[6] B. Kulicka, R. Jakubas, Z. Ciunik, G. Bator, W. Medycki, J. Świergiel and J. Baran, "Structure, phase transitions and molecular dynamics in 4-methylpyridinium tetrachloroantimonate (III), $(4\text{-}CH_3C_5H_4NH)(SbCl_4)$." *J. Phys. Chem. Solids*, vol. 65, pp. 871-879, 2004.

[7] C. B. Mohamed, K. Karoui, S. Saidi, K. Guidara and A. B. Rhaiem, "Electrical properties, phase transitions and conduction mechanisms of the $((C_2H_5)NH_3)_2CdCl_4$ compound. " *Physica B*, vol. 451, pp. 87-95, 2014.

[8] S. Kalyanaraman, P. M. Shajinshinu and S. Vijayalakshmi, "Refractive index, band gap energy, dielectric constant and polarizability calculations of ferroelectric Ethylenediaminium Tetrachlorozincate crystal." *J. Phys. Chem. Solids*, vol. 86, pp. 108-113, 2015.

[9] T. Baikie, Y. Fang, J. M. Kadro, M. Schreyer, F. Wei, S. G. Mhaisalkar, M. Graetzel and T. J. White, "Synthesis and crystal chemistry of the hybrid perovskite $(CH_3NH_3)PbI_3$ for solid-state sensitised solar cell applications." *J. Mater. Chem. A*, vol. 1, pp. 5628-5641, 2013.

[10] N. A. Benedek, J. M. Rondinelli, H. Djani, P. Ghosez and P. Lightfoot, "Understanding ferroelectricity in layered perovskites: new ideas and insights from theory and experiments." *Dalton Trans.,* vol. 44, pp. 10543-10558, 2015.

[11] Z. Cheng and J. Lin, "Layered organic–inorganic hybrid perovskites: structure, optical properties, film preparation, patterning and templating engineering." *CrystEngComm*, vol. 12, pp. 2646-2662, 2010.

[12] Y. Wei, P. Audebert, L. Galmiche, J. S. Lauret and E. Deleporte, "Synthesis, optical properties and photostability of novel fluorinated organic–inorganic hybrid $(R\text{–}NH_3)_2PbX_4$ semiconductors." *J. Phys. D: Appl. Phys.*, vol. 46, pp. 135105, 2013.

[13] K. Pradeesh, G. S. Yadav, M. Singh and G. V. Prakash, "Synthesis, structure and optical studies of inorganic–organic hybrid semiconductor, $NH_3(CH_2)_{12}NH_3PbI_4$." *Mater. Chem. Phys.*, vol. 124(1), pp. 44-47, 2010.

[14] N. V. Petrova and , I. N. Yakovkin "DFT calculations of the electronic structure of SnOx layers on Pd (110)." *Eur. Phys. J. B,* vol. 86, pp. 1-5, 2013.

[15] R. El Mrabet, S. Kassou, O., Tahiri, A., Belaaraj and P. Guionneau, "Theoretical and experimental investigations of optical, structural and electronic properties of the lower-dimensional hybrid $(NH_3\text{-}(CH_2)_{10}\text{-}NH_3)\ ZnCl_4$." *Eur. Phys. J. Plus*, vol. 131, pp. 369, 2016.

[16] C. E. Ekuma, V. I. Anisimov, J. Moreno and M. Jarrell, "Electronic structure and spectra of CuO." *Eur. Phys. J. B*, vol. 87, pp. 1-6, 2014.

[17] S. Kassou, A., Kaiba, P., Guionneau and A. Belaaraj, "Organic-inorganic hybrid perovskite $(C_6H_5(CH_2)_2NH_3)_2CdCl_4$: Synthesis, structural and thermal properties." *J. Struct. Chem.,* vol. 57, pp. 737-743, 2016.

[18] S. Naderizadeh, S. M. Elahi, M. R. Abolhassani, F. Kanjouri, N., Rahimi and J. Jalilian, "Electronic and optical properties of Full-Heusler alloy Fe3− xMnxSi." *Eur. Phys. J. B*, vol. 85, pp. 1-7, 2012.

[19] S. Sharma and A. S. Verma, "Structural, electronic, optical, elastic and thermal properties of $ZnXAs_2$ (X= Si and Ge) chalcopyrite semiconductors." *Eur. Phys. J. B*, vol. 87, pp. 1-14, 2014.

[20] R. Khenata, B. Daoudi, M. Sahnoun, H., Baltache, M. Rérat, A. H. Reshak, B. Bouhafs, H. Abid and M. Driz. "Structural, electronic and optical properties of fluorite-type compounds." *Eur. Phys. J. B*, vol. 47, pp. 63-70, 2005.

[21] I. C. Smith, E. T. Hoke, D. Solis-Ibarra, M.D. McGehee and H. I. Karunadasa, "A layered hybrid perovskite solar-cell absorber with enhanced moisture stability." *Angew. Chem. Int. Ed.*, vol. 126, pp. 11414-11417, 2014.

[22] C. G. Bischak, E. M., Sanehira, J. T. Precht, J. M. Luther and N. S. Ginsberg "Heterogeneous Charge Carrier Dynamics in Organic–Inorganic Hybrid Materials: Nanoscale Lateral and Depth-Dependent Variation of Recombination Rates in Methylammonium Lead Halide Perovskite Thin Films." *Nano letters*, vol. 15, pp. 4799-4807, 2015.

[23] M. A. Green, Y. Jiang, A. M. Soufiani and A. Ho-Baillie, "Optical Properties of Photovoltaic Organic–Inorganic Lead Halide Perovskites." *J. phys. Chem. Lett*., vol. 6, pp. 4774-4785. 2015.

[24] X. Liu, W. Zhao, H. Cui, Y. A. Xie, Y. Wang, T. Xu and F. Huang, "Organic–inorganic halide perovskite based solar cells–revolutionary

progress in photovoltaics." *Inorg. Chem. Front.*, vol. 2, pp. 315-335, 2015.
[25] N. G. Park, "Perovskite solar cells: an emerging photovoltaic technology." Mater. Today, vol. 18, pp. 65-72, 2015.
[26] Y. Zhao and K. Zhu, "Organic–inorganic hybrid lead halide perovskites for optoelectronic and electronic applications." Chem. Soc. Rev, vol. 45, pp. 655-689, 2016.
[27] L. Pedesseau, J. M. Jancu, A. Rolland, E. Deleporte, C. Katan and J. Even, "Electronic properties of 2D and 3D hybrid organic/inorganic perovskites for optoelectronic and photovoltaic applications." *J. Opt. Quant. Electron.*, vol. 46, pp. 1225-1232, 2014.
[28] C. Motta, F. El-Mellouhi and S. Sanvito,. "Charge carrier mobility in hybrid halide perovskites." *Sci. Rep*., vol. 5, 2015.
[29] S. M. B. Dhas and S. Natarajan, "Growth and characterization of two new NLO materials from the amino acid family: l-Histidine nitrate and l-Cysteine tartrate monohydrate." *Opt. Commun.,* vol. 281, pp. 457-462, 2008.
[30] J. J. Zhang, T. Zhang, Y. E. Jin, S. S. Liu, S. D. Yuan, Z. Cui, L. Zhang and W. H. Wang, "A tunable lighting system integrated by inorganic and transparent organic light-emitting diodes." *Optoelectron. Lett*., vol. 10, pp. 198-201, 2014.
[31] L. Wang, M. H. Yoon, G. Lu, Y. Yang, A., Facchetti and T. J. Marks, "High-performance transparent inorganic–organic hybrid thin-film n-type transistors." *Nat. Mater.,* vol. 5, pp. 893-900, 2006.
[32] S. Kassou, R. El-Mrabet, A. Kaiba, P. Guionneau and A. Belaaraj, "Combined experimental and density functional theory studies of an organic–inorganic hybrid perovskite." *Phys. Chem. Chem. Phys.*, vol. 18, pp. 9431-9436, 2016.
[33] W. Amamou, H. Feki, N. Chniba-Boudjada and F. Zouari, "Synthesis, crystal structure, vibrational properties and theoretical investigation of (N, N- dimethylbenzylammonium) trichlorocadmate (II)." *J. Mol. Struct.,*vol. 1059, pp. 169-175, 2014.
[34] A. Jellibi, I. Chaabane and K. Guidara, "Experimental and theoretical study of AC electrical conduction mechanisms of Organic–inorganic hybrid compound Bis (4-acetylanilinium) tetrachlorocadmiate (II)." *Physica E*, vol. 80, pp.155-162, 2016.
[35] B. Staśkiewicz, I. Turowska-Tyrk, J. Baran, C. Górecki and Z. Czapla, "Structural characterization, thermal, vibrational properties and molecular motions in perovskite-type diaminopropanetetrachlorocadmate $NH_3(CH_2)_3NH_3CdCl_4$ crystal." *J. Phys. Chem. Solid.*, vol. 75, pp. 1305-1317, 2014.
[36] R. Elwej, M. Hamdi, N. Hannachi and F. Hlel, "Synthesis, structural characterization and dielectric properties of $(C_6H_9N_2)_2(Hg_{0.75}Cd_{0.25})Cl_4$ compound." *Spectrochim. Acta Mol. Biomol.,* vol. 121, pp. 632-640, 2014.
[37] S. Kalyanaraman, V. Krishnakumar, H. Hagemann and K. Ganesan, "Infrared and polarized Raman spectra of dixanthinium tetrachlorozincate single crystal." *J. Phys. Chem. Solid*., vol. 68, pp. 256-263, 2007.
[38] P. Judeinstein and C. Sanchez, "Hybrid organic–inorganic materials: a land of multidisciplinarity." *J. Mater. Chem., vol*. 6, pp. 511-525, 1996.
[39] C. Sanchez, B. Lebeau, F. Chaput and J. P. Boilot, "Optical properties of functional hybrid organic–inorganic nanocomposites." Adv. Mater., vol. 15, pp. 1969-1994, 2003.
[40] C. Kitel, Introduction to solid state. John Wiley Sons, 1966.
[41] J. Tauc, Optical properties of amorphous semiconductors. In Amorphous and Liquid Semiconductors. Springer US, 1974, pp. 159-220.
[42] A. O. Polyakov, A. H. Arkenbout, J. Baas, G. R. Blake, A. Meetsma, A., Caretta, P. H. M. van Loosdrecht and T. T. M. Palstra, "Coexisting ferromagnetic and ferroelectric order in a $CuCl_4$-based organic–inorganic hybrid." *Chem. Mater.,* vol. 24, pp. 133-139, 2011.
[43] S. K. J. Al-Ani, Y. Al-Ramadin, M. S. Zihlif, M. Volpe, M. Malineonico, E. Martuscelli and G. Ragosta. " The optical properties of polymethylmethacrylate polymer dispersed liquid crystals". Polymer Testing, vol. 18, pp. 611-619, 1999.
[44] S. Ilican, M. Zor, Y. Caglar, and M. Caglar, " Optical characterization of the CdZn(S1-xSex)2 thin films deposited by spray pyrolysis method." Opt. Appl, vol. 36, pp. 29-37, 2006..
[45] F. E. Fernández, Y. González, H. Liu, A. Martínez, V. Rodríguez and W. Jia, "Structure, morphology, and properties of strontium barium niobate thin films grown by pulsed laser deposition." *Integr. Ferroelectr*., vol. 42, pp. 219-233, 2002.
[46] M. D. Catedral, A. K. G. Tapia, R. V. Sarmago, J. P. Tamayo and E. J. del Rosario, "Effect of dopant ions on the electrical conductivity and microstructure of polyaniline (emeraldine salt)." *Science Diliman*, Vol. 16(2), pp. 41-46, 2007.
[47] W. Li, Z. Chen, R. N. Premnath, B. Kabius and O. Auciello, "Controllable giant dielectric constant in AlOx/TiOy nanolaminates." *J. Appl. Phys.*, vol. 110, pp. 024106, 2011.
[48] Q. Li, L. Chen, M. R. Gadinski, S. Zhang, G. Zhang, H.Li, A. Haque, L-Q. Chen, T. Jackson and Q. Wang, "Flexible high-temperature dielectric materials from polymer nanocomposites." *Nature*, vol. 523, pp. 576-579, 2015.
[49] K. Maex, M.R. Baklanov, D. Shamiryan, S.H. Brongersma and Z.S. Yanovitskaya "Low dielectric constant materials for microelectronics." *J. Appl. Phys*., vol. 93, pp. 8793-8841, 2003.
[50] D. H. Fabini, T. Hogan, H. A. Evans, C. C. Stoumpos, M. G. Kanatzidis and R. Seshadri "Dielectric and thermodynamic signatures of low-temperature glassy dynamics in the hybrid perovskites $CH_3NH_3PbI_3$ and $HC(NH_2)_2PbI_3$." *J. Phys. Chem. Chem. Lett*., vol. 7, pp. 376-381, 2016.